Multi-octave linearized analog photonic link based on a polarization-multiplexing dual-parallel Mach-Zehnder modulator

Dan Zhu, Jian Chen, and Shilong Pan*

The Key Laboratory of Radar Imaging and Microwave Photonics, Ministry of Education, Nanjing University of Aeronautics and Astronautics, Nanjing 210016, China

*pans@ieee.org

Abstract: A multi-octave highly-linear analog photonic link with simultaneous suppression of second-order intermodulation distortion (IMD2) and third-order intermodulation distortion (IMD3) is proposed and demonstrated based on a single integrated polarization-multiplexing dual-parallel Mach-Zehnder modulator (PM-DPMZM). The IMD2 is eliminated by biasing one sub-MZM in each sub-DPMZM at a point close to the maximum transmission point and the other sub-MZM at a point close to the minimum transmission point. The obtained fundamental frequency terms are in phase while the second-order harmonics are complementary when the two outputs of the two sub-MZMs are photodetected. The IMD3 is suppressed by adjusting the RF powers introduced to the two sub-DPMZMs, producing two complementary IMD3 terms when the modulated signals are photodetected. An experiment is carried out. Simultaneous suppression of IMD2 and IMD3 is achieved. The second-order spurious-free dynamic range (SFDR2) and third-order spurious-free dynamic range (SFDR3) are 82 dB·Hz$^{1/2}$ and 110 dB·Hz$^{2/3}$, respectively, indicating an improvement of 12 dB in SFDR2 and 13 dB in SFDR3 as compared with the low-biased MZM based analog photonic link, or an improvement of 3 dB in SFDR2 and 16 dB in SFDR3 as compared with the quadrature-biased MZM based photonic link.

OCIS codes: (060.5625) Radio frequency photonics; (060.2360) Fiber optics links and subsystems; (070.1170) Analog optical signal processing.

References and links

1. J. Capmany and D. Novak, "Microwave photonics combines two worlds," Nat. Photonics **1**(6), 319–330 (2007).
2. P. Ghelfi, F. Laghezza, F. Scotti, G. Serafino, A. Capria, S. Pinna, D. Onori, C. Porzi, M. Scaffardi, A. Malacarne, V. Vercesi, E. Lazzeri, F. Berizzi, and A. Bogoni, "A fully photonics-based coherent radar system," Nature **507**(7492), 341–345 (2014).
3. A. J. Stark, K. Davis, C. Ward, and J. Gray, "Photonics for electronic warfare," in *Proceedings of Avionics, Fiber-Optics and Photonics Technology Conference* (IEEE, 2014), pp. 3–4.
4. J. Yao, "Microwave photonics," J. Lightwave Technol. **27**(3), 314–335 (2009).
5. C. Lim, A. T. Nirmalathas, K.-L. Lee, D. Novak, and R. Waterhouse, "Intermodulation distortion improvement for fiber–radio applications incorporating OSSB+ C modulation in an optical integrated-access environment," J. Lightwave Technol. **25**(6), 1602–1612 (2007).
6. Y. Shen, B. Hraimel, X. Zhang, G. E. Cowan, K. Wu, and T. Liu, "A novel analog broadband RF predistortion circuit to linearize electro-absorption modulators in multiband OFDM radio-over-fiber systems," IEEE Trans. Microw. Theory Tech. **58**(11), 3327–3335 (2010).
7. T. R. Clark and M. L. Dennis, "Coherent optical phase-modulation link," IEEE Photonics Technol. Lett. **19**(16), 1206–1208 (2007).
8. A. Karim and J. Devenport, "Low noise figure microwave photonic link," in *Proceedings of IEEE/MTT-S International Microwave Symposium* (IEEE, 2007), pp. 1519–1522.
9. M. Huang, J. Fu, and S. Pan, "Linearized analog photonic links based on a dual-parallel polarization modulator," Opt. Lett. **37**(11), 1823–1825 (2012).
10. S. Li, X. Zheng, H. Zhang, and B. Zhou, "Highly linear radio-over-fiber system incorporating a single-drive dual-parallel Mach–Zehnder modulator," IEEE Photonics Technol. Lett. **22**(24), 1775–1777 (2010).

#261776 Received 24 Mar 2016; revised 5 May 2016; accepted 5 May 2016; published 11 May 2016

11. D. Liang, Q. Tan, W. Jiang, Z. Zhu, X. Li, and Z. Yao, "Influence of Power Distribution on Performance of Intermodulation Distortion Suppression," IEEE Photonics Technol. Lett. **27**(15), 1639–1641 (2015).
12. W. Li and J. Yao, "Dynamic range improvement of a microwave photonic link based on bi-directional use of a polarization modulator in a Sagnac loop," Opt. Express **21**(13), 15692–15697 (2013).
13. P. Li, L. Yan, T. Zhou, W. Li, Z. Chen, W. Pan, and B. Luo, "Improvement of linearity in phase-modulated analog photonic link," Opt. Lett. **38**(14), 2391–2393 (2013).
14. A. Bhatia, H.-F. Ting, and M. A. Foster, "Linearization of phase-modulated analog optical links using a four-wave mixing comb source," Opt. Express **22**(25), 30899–30909 (2014).
15. X. J. Meng and A. Karim, "Microwave photonic link with carrier suppression for increased dynamic range," Fiber Integr. Opt. **25**(3), 161–174 (2006).
16. W. Burns, G. Gopalakrishnan, and R. Moeller, "Multi-octave operation of low-biased modulators by balanced detection," IEEE Photonics Technol. Lett. **8**(1), 130–132 (1996).
17. P. S. Devgan, J. F. Diehl, V. J. Urick, C. E. Sunderman, and K. J. Williams, "Even-order harmonic cancellation for off-quadrature biased Mach-Zehnder modulator with improved RF metrics using dual wavelength inputs and dual outputs," Opt. Express **17**(11), 9028–9039 (2009).
18. Y. Cui, K. Xu, Y. Dai, and J. Lin, "Suppression of second-order harmonic distortion in ROF links utilizing dual-output MZM and balanced detection," in *Proceedings of International Topical Meeting on Microwave Photonics* (IEEE, 2012), pp. 103–106.
19. S. L. Pan, D. Zhu, S. F. Liu, K. Xu, Y. T. Dai, T. L. Wang, J. G. Liu, N. H. Zhu, Y. Xue, and N. J. Liu, "Satellite Payloads Pay Off," IEEE Microw. Mag. **16**(8), 61–73 (2015).
20. R. Waterhouse and D. Novack, "Realizing 5G: Microwave Photonics for 5G Mobile Wireless Systems," IEEE Microw. Mag. **16**(8), 84–92 (2015).
21. D. M. Pozar, *Microwave Engineering* (Wiley, 2005).
22. C. H. Cox, *Analog Optical Links: Theory and Practice* (Cambridge University, 2006).
23. K. J. Williams, R. D. Esman, and M. Dagenais, "Nonlinearities in pin microwave photodetectors," J. Lightwave Technol. **14**(1), 84–96 (1996).
24. S. A. Malyshev and A. L. Chizh, "p-i-n photodiodes for frequency mixing in radio-over-fiber systems," J. Lightwave Technol. **25**(11), 3236–3243 (2007).

1. Introduction

Thanks to the advantages in terms of broad bandwidth, low loss, light weight, and immunity to electromagnetic interference, analog photonic link is considered a key technology for the distribution of RF signals with large bandwidth, which is required in applications such as the next generation wireless communication systems [1], radars [2] and electronic warfare [3]. An important performance indicator of the analog photonic link is the spurious-free dynamic range (SFDR) which is always limited by the nonlinear transfer function of the optical transmitter [4]. For a single-octave system, the third-order intermodulation distortion (IMD3) which is close to the spectrum of the signal for transmission is the main restriction factor of the SFDR, since the second-order intermodulation distortion (IMD2) and the second-order harmonic distortion (SHD) are out of the band of interest, which can be easily removed by a filter [5]. In the past decades, great efforts have been devoted to improve the SFDR of the analog photonic link by suppressing the IMD3 [5–15]. Electronic linearization including electrical predistortion [6] and post digital signal processing [7] is one typical way to suppress the IMD3, but it has limited bandwidth due to the electronic bottleneck. Another way to eliminate the IMD3 is to produce one complementary IMD3 term to cancel the existing one. Methods in this category include the use of two Mach-Zehnder modulators (MZMs) in parallel [8], dual-parallel polarization modulators [9], a dual-parallel Mach-Zehnder modulator (DPMZM) [10,11], or bidirectional operation of a polarization modulator [12]. However, precise matching of the parallel links is usually needed and hard to realize [8,9]. In [10], the optical carrier is modulated in one of the two parallel modulators and unmodulated in the other one, and IMD3 suppression is achieved by adjusting the three biases and the modulation depth. For the approach in [11], the optical carrier is modulated in both the two parallel modulators, and IMD3 suppression is achieved by the biases of the DPMZM and using a unsymmetrical power divider to adjust the modulation depth in both the two parallel modulators. For both the approaches, IMD2 suppression is not considered. Linearized photonic links based on phase modulation have also been proposed, taking the advantages of high degree of linearity and bias-free operation of the phase modulators [13,14]. However, extra optical bandpass filters are required, which makes the system complicated and restricts the frequency range. A low-biased MZM based analog photonic link has also been proposed

#261776 Received 24 Mar 2016; revised 5 May 2016; accepted 5 May 2016; published 11 May 2016

to improve the third-order spurious-free dynamic range (SFDR3) performance [15]. All the above approaches, however, can only be applied in single-octave photonic links, since only the IMD3 is suppressed while the IMD2 and SHD still exist.

On the other hand, some efforts have been devoted to suppress the IMD2 of the analog photonic link [16–18]. The key idea is to implement two intensity modulations, which would produce two complementary IMD2 if the modulated signals are sent to the photodetectors (PDs). This can be realized by placing two MZMs in parallel [16], employing the wavelength-dependent nature of the half-wave voltage of a $LiNbO_3$ modulator [17], and using a dual-output MZM followed by a balanced PD [18]. These systems are usually complicated since two lasers or two modulators are needed. In addition, all these approaches are only effective for the suppression of the IMD2, so the SFDR of the system is still limited. For future wireless communication (such as satellite communication [19], and 5G Mobile Wireless communication [20]) and military applications [2,3], RF signals with large bandwidth will be used and the system should be operated within multi-octave bandwidth. Not only the IMD3 but also the IMD2 and SHD will lie in the spectral range of interest, which cannot be simply filtered out. As a result, the simultaneous elimination of the IMD3, the IMD2 and the SHD are highly required.

In this paper, a multi-octave highly linear analog photonic link with simultaneous IMD2 and IMD3 suppression based on a polarization-multiplexing dual-parallel Mach-Zehnder modulator (PM-DPMZM) is proposed. Compared to the previously reported approaches to increase the SFDR of an analog photonic link, the proposed scheme eliminates the IMD2 and the IMD3 simultaneously by using only one laser diode (LD), one modulator and one PD. An experiment is carried out. Both the IMD2 and IMD3 of the proposed link are effectively suppressed. The second-order spurious-free dynamic range (SFDR2) and SFDR3 are measured to be 82 $dB\cdot Hz^{1/2}$ and 110 $dB\cdot Hz^{2/3}$, respectively, indicating that an improvement of 12 dB in SFDR2 and 13 dB in SFDR3 is achieved as compared with the low-biased MZM based photonic link, or an improvement of 3 dB in SFDR2 and 16 dB in SFDR3 as compared with the quadrature-biased MZM based photonic link.

2. Principle

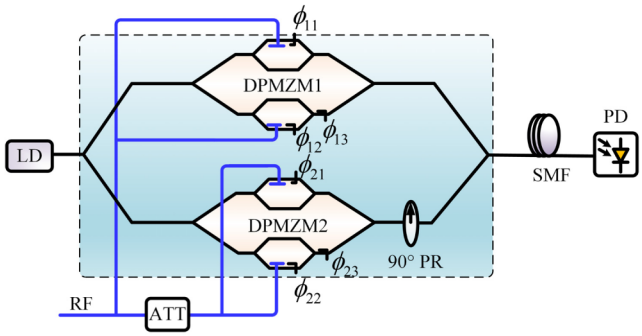

Fig. 1. Schematic diagram of the proposed linearized analog photonic link based on a polarization-multiplexing dual-parallel Mach-Zehnder modulator. LD: laser diode; DPMZM; dual parallel Mach-Zehnder modulator. PR: 90°polarization rotator; SMF: single mode fiber; PD: photodetector; ATT: microwave attenuator.

The schematic diagram of the proposed linearized analog photonic link based on a PM-DPMZM is shown in Fig. 1. A lightwave from a LD is introduced to a PM-DPMZM. The PM-DPMZM is an integrated modulator which is composed of two sub-DPMZMs lying in two branches and a 90°polarization rotator (PR) in one of the branchs. The lightwave is split into two parts and modulated at the two sub-DPMZMs. In the lower branch, the PR rotates the polarization state of the modulated signal by 90°to let it be orthogonal with the signal in

#261776 Received 24 Mar 2016; revised 5 May 2016; accepted 5 May 2016; published 11 May 2016

the upper branch. The two orthogonally polarized lightwaves are then combined at the output of the PM-DPMZM, which can be expressed as

$$\begin{bmatrix} E_{01} \\ E_{02} \end{bmatrix} = \begin{bmatrix} E_I e^{j\omega_c t} \cos\left(\frac{\phi_{11}+\phi_{1m}(t)}{2}\right) + E_I e^{j(\omega_c t+\phi_{13}} \cos\left(\frac{\phi_{12}+\phi_{1m}(t)}{2}\right) \\ E_I{}^{j\omega_c t} \cos\left(\frac{\phi_{11}+\phi_{1m}(t)}{2}\right) + E_I e^{j(\omega_c t+\phi_{23}} \cos\left(\frac{\phi_{22}+\phi_{1m}(t)}{2}\right) \end{bmatrix} \tag{1}$$

where E_I and ω_c are the amplitude and angular frequency of the input optical carrier, respectively. $\phi_{ij} = \pi V_{ij}/V_{i\pi}$ is introduced by the DC bias V_{ij} of the j^{th} sub-MZM in the i^{th} sub-DPMZM, and $V_{i\pi}$ is the half-wave voltage of the i^{th} sub-DPMZM (i = 1, 2, j = 1, 2, 3). $\phi_{im}(t) = \pi V_{im}(t)/V_{i\pi} = \beta_i V_m(t)$ is the modulating RF signal on the i^{th} sub-DPMZM. Since the two lightwaves are orthogonally polarized, after photodetection, the generated photocurrent is

$$\begin{aligned} I(t) = \left|E_{O1}\right|^2 + \left|E_{O2}\right|^2 = \Re\sum_{i=1}^{2}\Bigg[& E_I^2 \cos^2\left(\frac{\phi_{i1}+\phi_{im}(t)}{2}\right) + E_I^2 \cos^2\left(\frac{\phi_{i2}+\phi_{im}(t)}{2}\right) \\ & + 2E_I^2 \cos\phi_{i3} \cos\left(\frac{\phi_{i1}+\phi_{im}(t)}{2}\right)\cos\left(\frac{\phi_{i2}+\phi_{im}(t)}{2}\right)\Bigg] \end{aligned} \tag{2}$$

where $\Re$ is the responsivity of the PD. Ignoring the DC term and setting $\phi_{i3} = k\pi + \pi/2$ and $\phi_{i2} = (2n + 1)\pi - \phi_{i1}$, where k and n are integers, Eq. (2) can be rewritten as

$$I(t) = -\Re E_I^2 \sin\phi_{11} \sin\phi_{1m} - \Re E_I^2 \sin\phi_{21} \sin\phi_{2m} \tag{3}$$

To evaluate the dynamic range performance of the link, a two-tone analysis should be applied, in which the RF signals with frequencies of ω_1 and ω_2 are applied. Setting $V_m(t) = \cos(\omega_1 t) + \cos(\omega_2 t)$, we get

$$\begin{aligned} I(t) &= -\Re E_1^2 \sin\phi_{11} \sin[\beta_1 \cos(\omega_1 t) + \beta_1 \cos(\omega_2 t)] - \Re E_2^2 \sin\phi_{21} \sin[\beta_2 \cos(\omega_1 t) + \beta_2 \cos(\omega_2 t)] \\ &= -\Re E_1^2 \sin\phi_{11} \left\{ \sum_{p=-\infty}^{p=+\infty} \sum_{q=-\infty}^{q=+\infty} J_p(\beta_1) J_q(\beta_1) \sin\left[p\omega_1 + q\omega_2 + (p+q)\pi/2\right] \right\} \\ &\quad - \Re E_2^2 \sin\phi_{21} \left\{ \sum_{p=-\infty}^{p=+\infty} \sum_{q=-\infty}^{q=+\infty} J_p(\beta_2) J_q(\beta_2) \sin\left[p\omega_1 + q\omega_2 + (p+q)\pi/2\right] \right\} \\ &= \sum_{i=1}^{2} \left\{ \Gamma_{i0} + \Gamma_{i1}\left[\cos(\omega_1 t) + \cos(\omega_2 t)\right] + \Gamma_{i3}\left[\cos(2\omega_1 - \omega_2) + \cos(2\omega_2 - \omega_1)\right] + \cdots \right\} \end{aligned} \tag{4}$$

where $J_n(\beta_i)$ donates the n^{th}-order Bessel function of the first kind, $\Gamma_{i1} = -\Re E_I^2 \sin\phi_{i1} J_0(\beta_i) J_1(\beta_i)$, and $\Gamma_{i3} = \Re E_I^2 \sin\phi_{i1} J_1(\beta_i) J_2(\beta_i)$. As can be seen, the IMD2 and SHD is eliminated. So Eq. (4) can be rewritten as

$$\begin{aligned} I(t) \propto \Re E_I^2 \{ & \left[-\sin\phi_{11} J_0(\beta_1) J_1(\beta_1) - \sin\phi_{21} J_0(\beta_2) J_1(\beta_2)\right]\left[\cos(\omega_1 t) + \cos(\omega_2 t)\right] + \\ & \left[\sin\phi_{11} J_1(\beta_1) J_2(\beta_1) + \sin\phi_{21} J_1(\beta_2) J_2(\beta_2)\right]\left[\cos(2\omega_1 - \omega_2) + \cos(2\omega_2 - \omega_1)\right] + \cdots \} \end{aligned} \tag{5}$$

From Eq. (5),the IMD3 can also be cancelled when the following condition is satisfied, i.e.

$$\begin{cases} -\sin\phi_{11} J_1(\beta_1) J_2(\beta_1) = \sin\phi_{21} J_1(\beta_2) J_2(\beta_2) \\ -\sin\phi_{11} J_0(\beta_1) J_1(\beta_1) \neq \sin\phi_{21} J_0(\beta_2) J_1(\beta_2) \end{cases} \tag{6}$$

#261776 Received 24 Mar 2016; revised 5 May 2016; accepted 5 May 2016; published 11 May 2016

By carefully adjusting the biases of the PM-DPMZM to make "$\phi_{i3}=k\pi+\pi/2$" and "$\phi_{i2}=(2n+1)\pi-\phi_{i1}$" which are expressed above (k and n are integers), and by adjusting the input RF power and the microwave attenuator to tune the β_1 and β_2 to make the condition in Eq. (6) to be satisfied, all the IMD2, SHD and IMD3 can be eliminated

Furthermore, for the small signal modulation condition, by adopting $J_n(m) \approx m^n/(2^n n!)$, Eq. (6) can be further simplified as

$$\begin{cases} -\sin\phi_{11}/\sin\phi_{21} = \beta_2^3/\beta_1^3 \\ -\sin\phi_{11}/\sin\phi_{21} \neq \beta_2/\beta_1 \end{cases} \tag{7}$$

Thus by adjusting the biases of the PM-DPMZM and the modulated RF power in both the two branches, a multi-octave linearized analog photonic link will be realized, with all the IMD2, SHD and IMD3 being eliminated.

3. Experimental results and discussions

An experiment based on the setup shown in Fig. 1 is carried out. The wavelength of the laser source (Teraxion, PS-NLL-1550.52-80-04) is set to be 1550.52 nm. The PM-DPMZM (Fujitsu FTM7977HQA) has a half-wave voltage of 3.5 V and a bandwidth of 23 GHz. In order to compare the link performance with the conditional MZM-based analog photonic links, a MZM (Fujitsu FTM7938EZ) with a 2.8-V half-wave voltage and a bandwidth of 25 GHz is used. The two-tone RF signal with frequencies of 17.995 GHz and 18.005 GHz is generated by a microwave signal generator (Angilent E8267D). A tunable microwave attenuator is used in one branch to adjust the power of the RF signal. The PD (u^2t, XPDV2150R) has a bandwidth of 50 GHz and a responsivity of 0.65 A/W. The electrical spectra are measured by an electrical signal analyzer (R&S, FSV-40, 10 Hz~40 GHz).

The link performances are measured by a two-tone signal test. As a comparison, the performance of the traditional links based on a quadrature-biased MZM and a low-biased MZM are also measured. Figure 2 shows the measured electrical spectra for all the three links when the total input RF power is set to be 6 dBm. By introducing a two-tone RF signal with frequencies of 17.995 and 18.005 GHz to the modulators, IMD3 components at frequencies of 17.985 GHz and 18.015 GHz are presented, as shown in Figs. 2(a)-2(c). Simultaneously, the SHD at frequencies of 35.99 and 36.01 GHz and the IMD2 at frequency of 36 GHz are also generated, with the spectra shown in Figs. 2(d)-2(f). In order to show the fundamental to IMD3 ratio differences for the three conditions more clearly, the output fundamental signal powers are set to be the same (about −37.5 dBm) by adjusting the optical powers injected into the PDs for the three conditions. As can be seen, linearization of the link is realized based on the PM-DPMZM. The fundamental to IMD3 ratio is dramatically increased to 55 dB, showing a 25-dB improvement as compared with the quadrature-biased MZM based photonic link, and a 20-dB improvement as compared with the low-biased MZM based photonic link. In addition, the measured power of the IMD2 component at 36 GHz for the proposed link is −78.2 dBm. Compared with the value of −70 dBm for the traditional quadrature-biased MZM based photonic link, the IMD2 cancellation ratio is about 8 dB, and compared with the value of −51.1 dBm for the low-biased MZM based photonic link, the IMD2 component is reduced by about 27 dB. According to [21], the SHD component is theoretically 6-dB lower than the corresponding IMD2 component, so all the IMD3, SHD and IMD2 are effectively suppressed in the proposed scheme. Figure 2(g) shows the measured electrical spectrum with a span of 24 GHz obtained by the proposed linearized link based on the PM-DPMZM, showing that multi-octave operation is achievable.

#261776 Received 24 Mar 2016; revised 5 May 2016; accepted 5 May 2016; published 11 May 2016

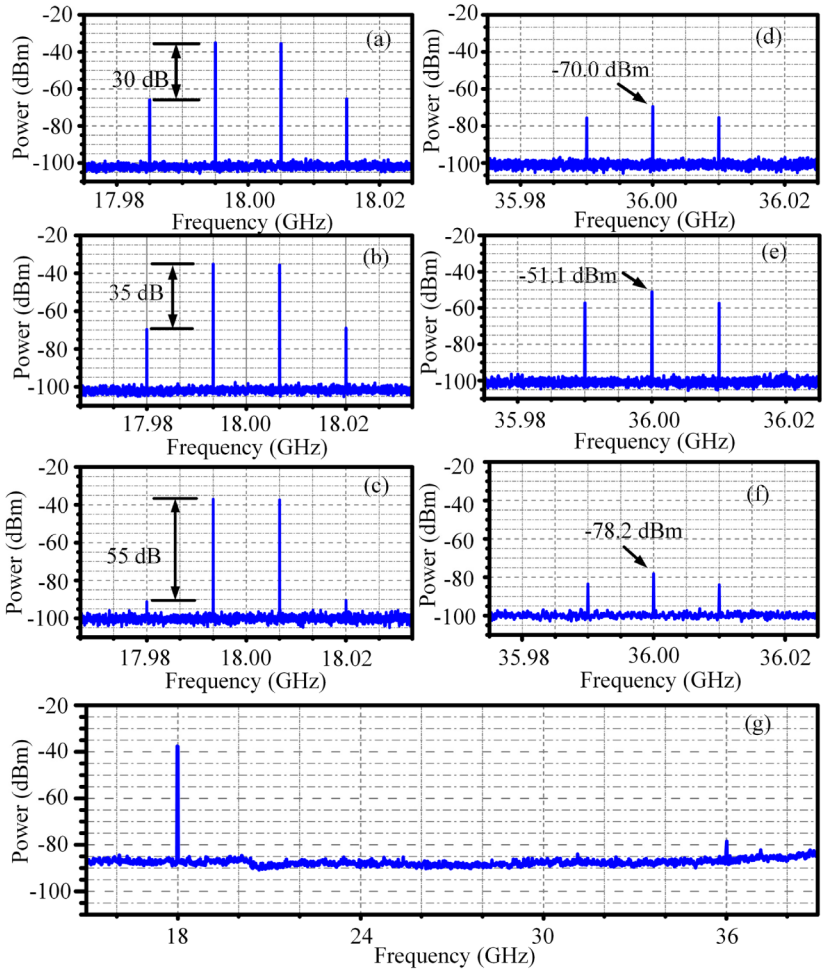

Fig. 2. Electrical spectra of the output fundamental signal and their IMD3 for (a) the quadrature-biased MZM, (b) the low-biased MZM and (c) the proposed PM-DPMZM based photonic links; Electrical spectra of the output SHD and IMD2 for (d) the quadrature-biased MZM, (e) the low-biased MZM and (f) the proposed PM-DPMZM based photonic links; (g) electrical spectrum with a span of 24 GHz for the proposed linearized photonic link based on the PM-DPMZM.

The SFDR performances are also measured by varying the input RF power. Considering the fixed 6-dB difference between the IMD2 and the SHD, IMD2 is used to calculate the SFDR2. For the comparison, Figs. 3(a) and 3(b) show the measured fundamental, IMD2 and IMD3 power as a function of the input RF power for the cases of the traditional photonic links based on the quadrature-biased MZM and the low-biased MZM, respectively. Figure 4 shows the measured fundamental, IMD2 and IMD3 powers as a function of the input RF power for the proposed linearized photonic link based on the PM-DPMZM, and the noise floor is set to be −160 dBm/Hz, according to the measurement. As can be seen, by using the proposed approach, the SFDR2 and SFDR3 are 82 dB·Hz$^{1/2}$ and 110 dB·Hz$^{2/3}$, respectively. Furthermore, the slope of the detected power at frequencies of 17.985 GHz and 18.015 GHz varying with the input RF power is 5, instead of 3 in traditional links, showing that IMD3 is almost eliminated and the main odd-order intermodulation distortions (IMDs) are originated from the fifth-order nonlinearity. On the other hand, the slope of the detected power at 17.985 and 18.015 GHz varying with the input RF power for both the quadrature- and low-biased MZM based photonic links is 3, confirming that their odd-order IMDs are generated by the

#261776 Received 24 Mar 2016; revised 5 May 2016; accepted 5 May 2016; published 11 May 2016

third-order nonlinearity. For the link based on PM-DPMZM, an improvement of 12 dB in SFDR2 and 13 dB in SFDR3 is achieved compared with the low-biased MZM based photonic link. The SFDR3 and SFDR2 of the quadrature-biased MZM based photonic link is 94 $dB \cdot Hz^{2/3}$ and 79 $dB \cdot Hz^{1/2}$, respectively. Compared with the quadrature-biased MZM based photonic link, the SFDR3 is improved by 16 dB, and the SFDR2 is improved by 3 dB. Thus it can be seen that by using the proposed scheme, the distortions of SHD, IMD2 and IMD3 can be cancelled simultaneously. In this way, the multi-octave operation is guaranteed.

In our experiments, the quadrature-biased MZM based photonic link is measured as a comparison, with the SFDR2 value of about 79 $dB \cdot Hz^{1/2}$. Theoretically, the IMD2 should be zero for the quadrature-biased MZM based photonic link [22]. However, in actual experiments, the ideal quadrature-biased working condition is affected by the enviroment, and the amplitude and phase relationships among the optical carriers and sidebands are changed, which in turn makes the system deviate from the ideal state with the IMD2 being equal to zero. In addition, the nonlinearities of the PDs will also result in the generation of IMD2 [23,24]. For the quadrature- and low-biased MZM based photonic links, the SFDR3 difference is 4 dB, which is mainly due to injected optical power differences into the PD [15].

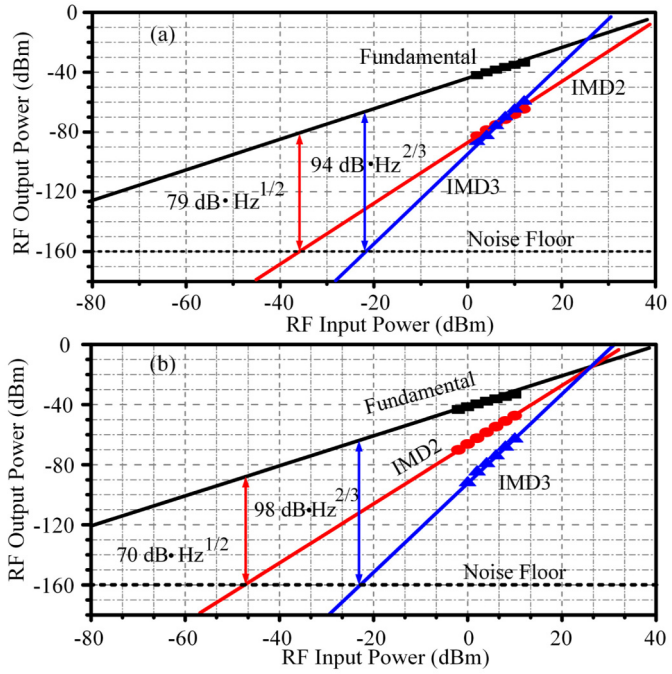

Fig. 3. SFDR performance of the (a) quadrature-biased and (b) low-biased MZM based photonic links.

#261776 Received 24 Mar 2016; revised 5 May 2016; accepted 5 May 2016; published 11 May 2016

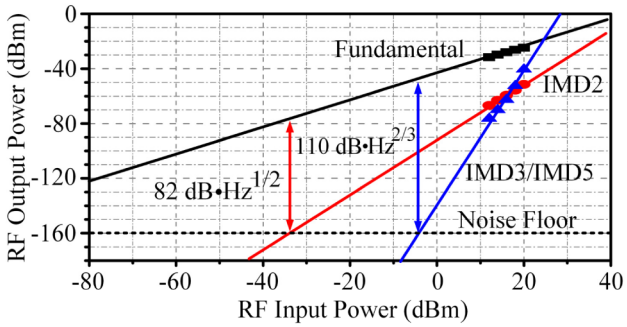

Fig. 4. SFDR performance of the proposed multi-octave linearized link based on the PM-DPMZM.

By using the proposed scheme, a multi-octave highly linear analog photonic link with simultaneous suppression of IMD2 and IMD3 is realized by using a single PM-DPMZM.The influence factors of the IMD2 and IMD3 suppression performance are mainly the modulator biases control stability and the modulated RF power tuning accuracy. The system performance can be further improved if stable bias voltage controllers are used and the RF power attenuator can realize tuning of the modulated RF signal's power more accurately. By integrating the RF power anttenuator in the modulator, the structure will be made simpler and the system performance will be improved.

4. Conclusion

We proposed and demonstrated a multi-octave highly linear analog photonic link with simultaneous suppression of IMD2 and IMD3 based on a single integrated PM-DPMZM. The proposed link requires only one LD, one modulator and one PD, which insures compact structure and simple operation. The simultaneous suppression of IMD2 and IMD3 is experimentally demonstrated, with SFDR2 and SFDR3 improved to 82 dB·$Hz^{1/2}$ and 110 dB·$Hz^{2/3}$, respectively. The IMD3 is effectively eliminated and the IMD5 is the main odd-order IMDs. The performance is improved by 12 dB in SFDR2 and by 13 dB in SFDR3 when compared with the low-biased MZM based analog photonic link, or improved by 3 dB in SFDR2 and 16 dB in SFDR3 as compared with the traditional quadrature-biased MZM based photonic link. The simultaneous elimination of IMD2 and IMD3 ensures multi-octave working bandwidth with linearity. This approach can find applications in future wireless communication systems and military systems.

Acknowledgements

This work was supported in part by the National Basic Research Program of China (2012CB315705), the Aviation Science Foundation of China (2013ZC52040), and the Fundamental Research Funds for Central Universities (NS2016037).

#261776 Received 24 Mar 2016; revised 5 May 2016; accepted 5 May 2016; published 11 May 2016